

## Radar observations of space debris

R. M. Goldstein,<sup>1</sup> S. J. Goldstein, Jr.<sup>2</sup> and D. J. Kessler<sup>3</sup>

<sup>1</sup>Jet Propulsion Laboratory, California Institute of Technology, 4800 Oak Grove Dr., Pasadena, CA 91109, U.S.A.

<sup>2</sup>Department of Astronomy, University of Virginia, P.O. Box 3818, Charlottesville, VA 22903, U.S.A.

<sup>3</sup>507 S. Shadowbend Rd., Friendswood, TX 77546, U.S.A.

**Abstract.** Our radar monitoring of small Earth-orbiting debris at NASA's Goldstone Tracking Station has been extended to an altitude of 3200 km. Many of the observed particles lie in clusters; the largest of which appears to be remnants of the West Ford Needles, launched over 3 decades earlier, and originally designed to have reentered the Earth's atmosphere long ago. © 1998 Elsevier Science Ltd. All rights reserved

### Introduction

Orbiting debris is recognized as a present and growing hazard for both humans and machines in space. Space collisions can have a closing velocity of  $15 \text{ km s}^{-1}$ , and even small particles are a serious safety concern. Knowledge of the changing environment of debris is necessary for both space mission design and for the assessment of debris mitigation policies.

Currently, the United States Space Command (Johnson 1993) maintains a catalog of orbital elements of space objects larger than about 10 cm. Monitoring of the flux of smaller objects has been accomplished by routine ground-based optical (Potter 1995) and radar observations (Stansbery, *et al* 1993). Very small particles of orbiting debris have also been detected *in situ* by spacecraft (Mandeville and Berthaud 1995), which have subsequently returned to Earth.

Occasionally, a 3.5 cm radar at NASA's Goldstone tracking station is available for orbital debris observations. This powerful radar, which can detect a conducting sphere of 3 mm diameter orbiting at an altitude of 1000 km, helps to fill an observational gap in the ongoing debris survey (Goldstein and Randolph 1992, and Goldstein and Goldstein 1994 and 1995).

### Observations

We report here the results of the Goldstone observations for seven runs between October, 1994, and March, 1996. The radar configuration was the same as reported previously, except that the maximum range was extended to 3200 km by increasing the listening period between transmitted pulses.

The transmitted pulses were increasing (or decreasing) frequency ramps of 51 kHz. Up-chirps alternated with down-chirps. Each pulse lasted for 2.3 ms and was followed by 0.2 ms of dead time and 20 ms of receive time. This arrangement permits the separate measurement of range and range-rate, provided that only one object at a time is in the beam. A typical particle of orbital debris at 1200 km altitude remains in the radar half-power beam for about 90 ms, thereby experiencing 4 pulses of illumination. No attempt was made to track the particles; the antennas were not moved.

Two antennas were used: a 70 m dish for the transmitter and a 35 m dish for the receiver. These antennas are separated by 497 meters along a line bearing 154.6 degrees from north. The larger, transmitting antenna was aimed 1.50 degrees from the zenith, towards the back of the receiving antenna. The receiving antenna, which could maintain pointing accuracy closer to the zenith, was aimed 1.44 degrees from the zenith, and along the same azimuth. The geometry for the pointing is given in Fig. 1, where the lower beam half-power intersection is shown at 280 km altitude, and the upper intersection at about 3000 km. The location of the upper intersection is a very sensitive function of antenna pointing.

As can be seen, the capture cross-section of the radar is a function of range and direction of the debris motion. Additionally, larger particles that do not cross the beam intersection can be detected through the antenna side-lobes. Such particles can usually be identified because they produce echoes over a longer time interval than the nominal duration of a main-beam crossing.

The observations dates and times are summarized in Table 1.

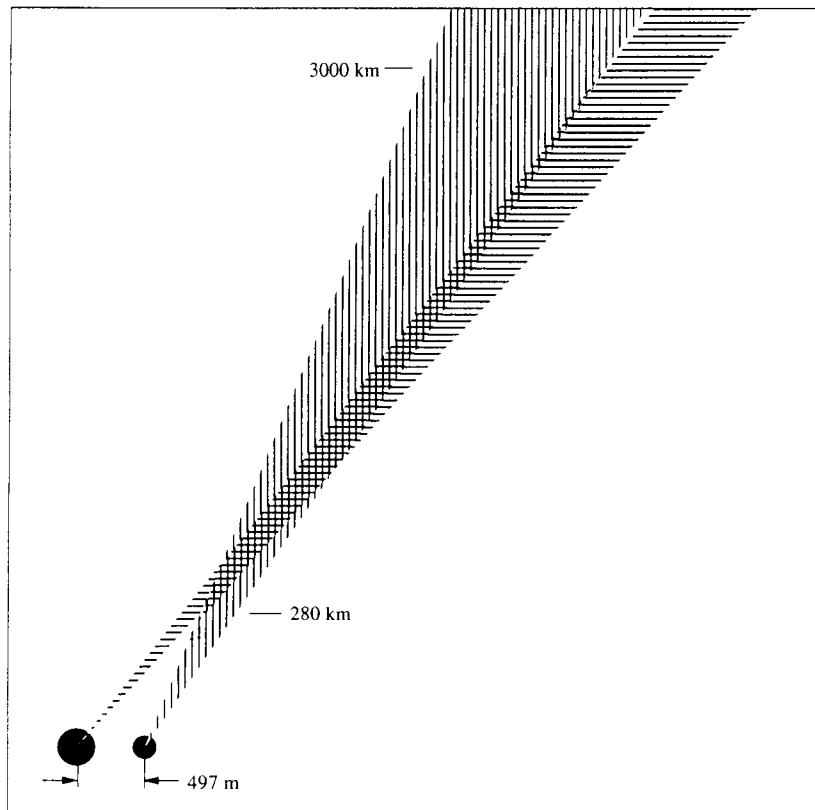


Fig. 1. Location and beam intersection geometry of transmitting and receiving antennas

Table 1.

Date	Hours, GMT	Hits
Oct 17, 1994	07.384-10.969	119
Oct 24, 1994	03.593-10.407	292
Nov 4, 1994	05.784-12.978	194
Dec 5, 1994	03.002-08.583	135
Nov 13, 1995	08.037-13.860	174
Nov 14, 1995	09.238-10.923	59
Mar 11, 1996	22.349-06.105	151

## Data

There were 1124 detections over 38.4 h of observations. A detection is defined as a threshold crossing on both the up- and down-chirp responses. The threshold was chosen such that noise alone could produce a false detection on an average of once per 28 h.

Most of the detections are likely to have been from particles crossing the main beam, as they persisted over the nominal beam time. However, 65 of the observed events lasted over a longer interval of time. These have been deemed side-lobe crossings, and have been removed from the data set.

Figure 2 presents the main-beam cumulative results, where particle effective diameter is plotted as a function of range. Effective diameter is defined as the diameter of a conducting sphere which would return the same power, at the same distance, as was actually measured.

The particles were assumed to pass through the center of the main antenna beam, and the measured power was corrected for the pattern of the smaller antenna. Effective diameter is computed from the measured radar cross section according to either the geometric cross section for larger particles or the Rayleigh approximation for small particles.

$$\sigma = \frac{\pi d^2}{4}, \quad \text{for larger particles} \quad (1a)$$

$$\sigma = \frac{d^6 \pi^5}{\lambda^4}, \quad \text{for smaller particles.} \quad (1b)$$

where  $\sigma$  is the radar cross section,  $\lambda$  is the wavelength and  $d$  is the effective diameter.

The lower limit seen in Fig. 2 is the result of the echo power being below the detection threshold; there appears to be a genuine lack of larger particles at the lower altitudes.

Figure 3 presents the line-of-sight velocity, as a function of range, for the main-beam detections. Positive velocities are for approaching particles. The system bandwidth permitted detection of particles with line-of-sight velocities between  $\pm 810 \text{ m s}^{-1}$ . Any particles with greater velocity have been filtered out by the detection system. A velocity of half of that limit would cause half of the received energy to be lost. A correction has been made to the radar cross section for this effect.

The Goldstone radar normally transmits right-hand circular polarization and receives the opposite sense. During

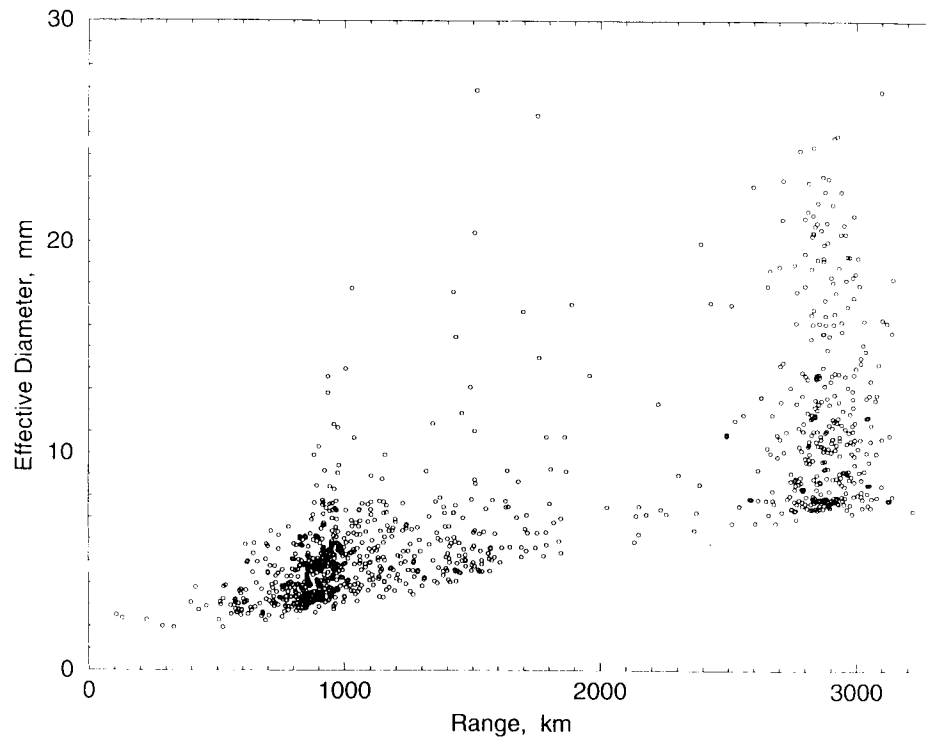


Fig. 2. Results of 38.4 h of observations, effective diameter vs range. Because the beams no longer intersect, the radar loses sensitivity rapidly below 300 km

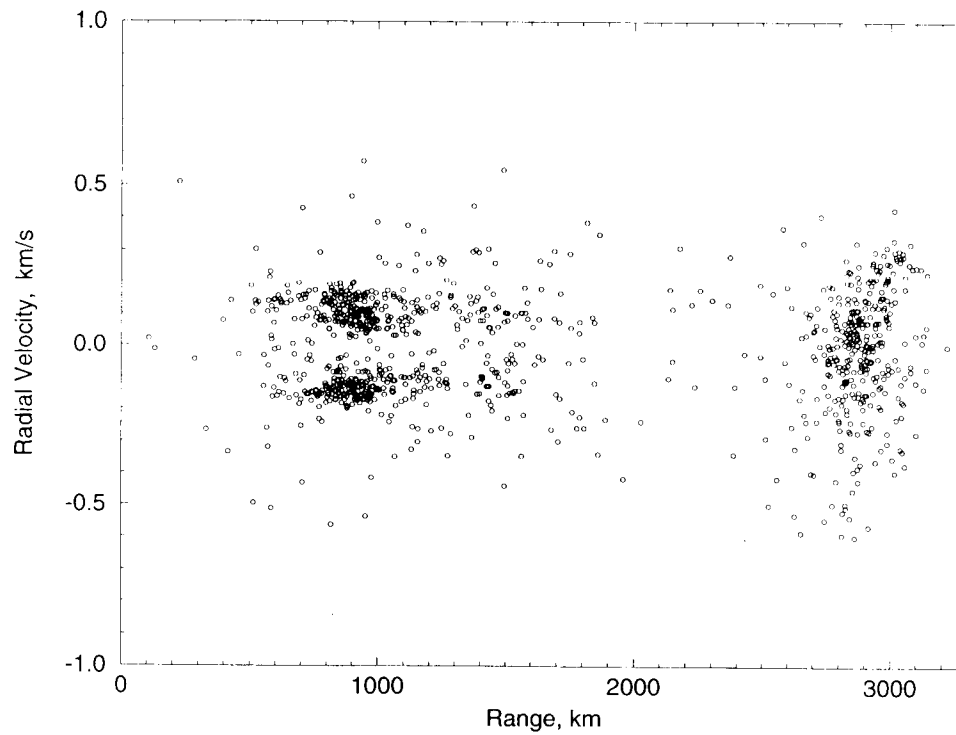


Fig. 3. Results, line-of-sight velocity vs range

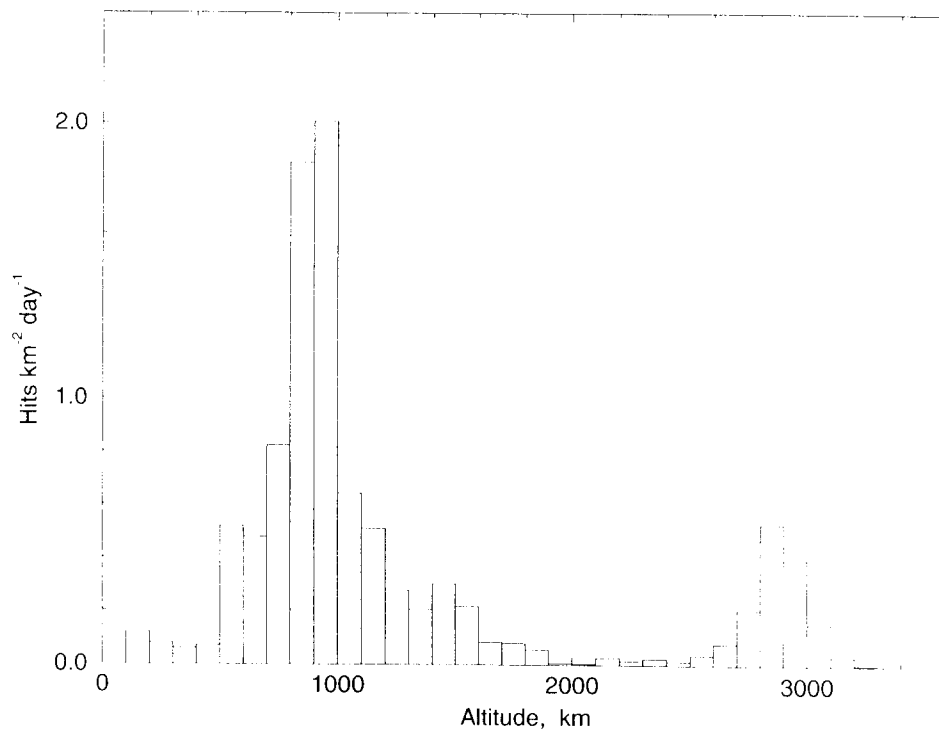


Fig. 4. Measured flux of small particle space debris

one hour, when the detection rate was high, the receiver polarization was reversed. The effects of this change will be noted subsequently.

### Flux

All of the data were sorted into 100 km altitude bins and normalized by the main-beam geometric cross section (i.e., the area shown in Fig. 1), and by the number of days of observation. The resulting flux measurements are given in Fig. 4. Most, but not all, of the flux of Fig. 4 represents objects in the millimetric range.

There is a peak in the flux histogram near 900 km. It has been previously observed by the Haystack (Stansbery *et al* 1995), and Goldstone (Goldstein and Goldstein 1995) radars. There is a second peak near 2900 km, not previously reported in radar measurements from the ground.

Figures 2, 3 and 4 show that much of the space debris population exists in range and radial-velocity clusters, which suggests common origins for them. We will discuss possible origins for both clusters in the following sections.

### Near cluster

The two clusters of points at ranges between 740 and 1020 km, shown in Fig. 3, appear to be observations of the same family of objects, seen once on the ascending portion of their orbits, and seen again on the descending portion.

Under the one-family, circular orbit assumptions, we can calculate the inclination of the orbits from the velocity ratio of the clusters. The velocities are projections, as follows:

$$v_1 \propto \cos(\beta - z); \quad \text{ascending} \quad (2a)$$

$$v_2 \propto \cos(\beta + z); \quad \text{descending} \quad (2b)$$

where  $z$  is the azimuth of the ascending pass, and  $\beta$  is the pointing azimuth of the antennas.

The orbital inclination is then determined by the solution for  $z$  and the known station latitude, with a small correction to  $z$  occasioned by the rotation of the Earth. The resulting inclination is  $70 \pm 5$  degrees. The uncertainty is estimated from the spread within the clusters. For a polar orbit, the two velocity clusters would coalesce. For an inclination greater than 90 degrees, the magnitude of the receding cluster velocity would be less than that of the approaching one.

During our hour-long experiment on polarization reversal, the detection rate for particles in the 740–1020 km altitude range dropped to 4 events per hour from an average of 10.8 events per hour.

Stansbery, *et al* (1995), and Kessler, *et al* (1995), have discussed radar observations at 3 cm for altitudes between 850 and 1000 km. They calculated an average orbital inclination of  $65^\circ$ , and referred to observations at Haystack that show that the particles do not reflect the orthogonal circular polarization. They concluded that the particles are spheres with diameters between 0.6 and 2 cm and that 70,000 are in orbit. These data led them to identify the source of the near cluster particles as the RORSAT satellite family. These satellites use a mixture of sodium and potassium in liquid form to cool their nuclear power supplies. Stansbery, *et al* (1995), adopt the hypothesis that the coolant leaks to form the spherical particles.

Our measurements show that the clustering in altitude near 900 km extends to particles at least as small as 0.25 cm diameter. The calculation of orbital inclination above

is in agreement with that of Stansbery, *et al* (1995). Our data leads to the inference of an additional population of 500,000 particles with diameters between 0.25 and 0.6 cm.

### Distant cluster

These particles, seen in Figs 2 and 3, have radar cross sections from 27 mm<sup>2</sup> at detection threshold, to a maximum observed of 466 mm<sup>2</sup>. They cluster in the altitude range between 2500 and 3100 km. They also show a marked clustering in time, which we show as histograms in Fig. 5. We estimate that there are 40,000 of these particles in orbit.

### Average orbital constants

Previously (Goldstein and Goldstein 1994, 1995), we have found average semi-major axes and eccentricities for groups of space-debris particles from least-square analysis of observed ranges and Doppler shifts at the zenith. The present observations, however, were made 1.5° away from the zenith. The measured range no longer adds directly to the geocentric radius to give the orbital radius, and the Doppler shift is not just the time derivative of the orbital radius for it now contains a small component of the orbital velocity.

However, we have found two long runs of observations where the Doppler shifts were nearly all of the same sense. One group with inward motion is listed in Table 2a the other, with outward motion, is listed in Table 2b.

We assume that a constant velocity correction will eliminate the orbital motion in each group, leaving range-rate

**Table 2a.** October 17, 1994 observations

GMT (hours)	Range (km)	Velocity (km s <sup>-1</sup> )
08:0956	2875.9	0.1830
08:1044	2674.5	0.0341
08:1594	2844.6	0.0466
08:1825	3022.3	0.2835
08:2022	2858.1	0.1146
08:2181	2961.0	0.1469
08:2378	2933.2	0.2075
08:2467	2914.7	0.2057
08:3019	2822.4	0.0723
08:3181	2790.0	0.0283
08:3475	2794.0	0.0580
08:3581	2868.3	0.1413
08:3819	2849.9	0.1126
08:4222	2848.6	0.1987
08:4364	2902.4	0.1478
08:4706	2616.4	0.1231
08:4839	2760.7	-0.1523
08:5181	2809.1	0.0227
08:5389	2952.2	0.2360
08:5583	2845.7	0.0955
08:5608	2794.6	0.0031
08:6133	3040.1	0.2817
08:6189	2760.5	0.0041
08:6472	2778.1	-0.0048

**Table 2b.** November 4, 1994 observations

GMT (hours)	Range (km)	Velocity (km s <sup>-1</sup> )
07:8386	2892.1	-0.1639
07:8781	2927.0	-0.2523
07:8822	2905.1	-0.0815
07:9136	2931.9	0.0109
07:9467	2923.4	-0.1824
07:9586	2942.0	-0.1068
07:9900	2917.3	-0.2693
08:0647	2922.7	0.0439
08:1208	2889.6	0.0629
08:1450	2816.1	-0.0840
08:1506	2926.7	-0.0451
08:1800	2993.5	0.0777
08:5983	2864.1	-0.3488
08:6381	3044.0	0.0125
08:8894	2883.5	-0.0394
09:3064	2946.1	0.0913
09:5842	2919.6	-0.0014
09:6286	2990.2	0.0051

as it would be seen from the Earth's center. We use the method of least-squares to find the constants that minimize the squared residuals of the solutions for  $a$  and  $e$ . For the first group, the constant is  $-0.08$  km s<sup>-1</sup>; for the second,  $+0.15$  km s<sup>-1</sup>. Both constants reduce the absolute value of the velocities, a result that is consistent with the above assumption.

The corresponding semi-major axes and eccentricities are, for the observations in Table 2a,  $a = 9285 \pm 148$  km and  $e = 0.0204 \pm 0.0097$ , where the errors represent one standard deviation. For Table 2b,  $a = 9405$  km  $\pm 116$  km and  $e = 0.0220 \pm 0.0070$ . There is good agreement between these values and we adopt the mean values  $a = 9345$  km and  $e = 0.0212$ .

From the average semi-major axis and the assumption of zero eccentricity, we can find from the data in Fig. 5 an estimate of the precession of the orbital node for a single orbiting cluster. A straight line fitted to the four peaks gives a precession of  $+6.0 \pm 0.5$  h per year, a value which corresponds (Danby 1962) to an inclination of  $95.5 \pm 1^\circ$  for the cluster. We estimate that the error in cluster arrival time to be about 1/2 of the observation window.

### Properties of known debris in the altitude range 2500 to 5000 km

In order to find a source for this debris, we have searched Molezan's (1997) very extensive catalogue of orbital elements of (almost) all satellites still in Earth orbit. The results are given in Fig. 6, where altitude is plotted against inclination. The dotted line represents the  $\pm 1$  degree uncertainty, and accounts for the fact that the inclination calculation depends upon the altitude. Only one spacecraft is a reasonable source of the debris—Midas 4.

On October 21, 1961, the West Ford Project, using Midas 4, attempted to place 350 million copper dipoles into a 3500 by 3800 km, 96 degree inclination orbit, as a

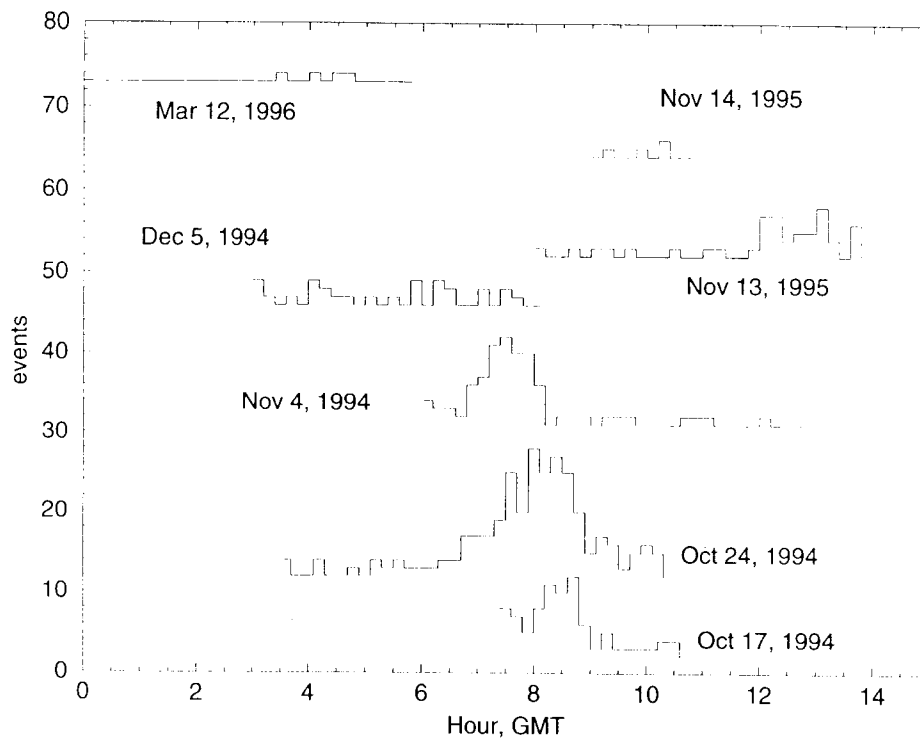


Fig. 5. Histograms of times of arrival for the distant cluster of debris

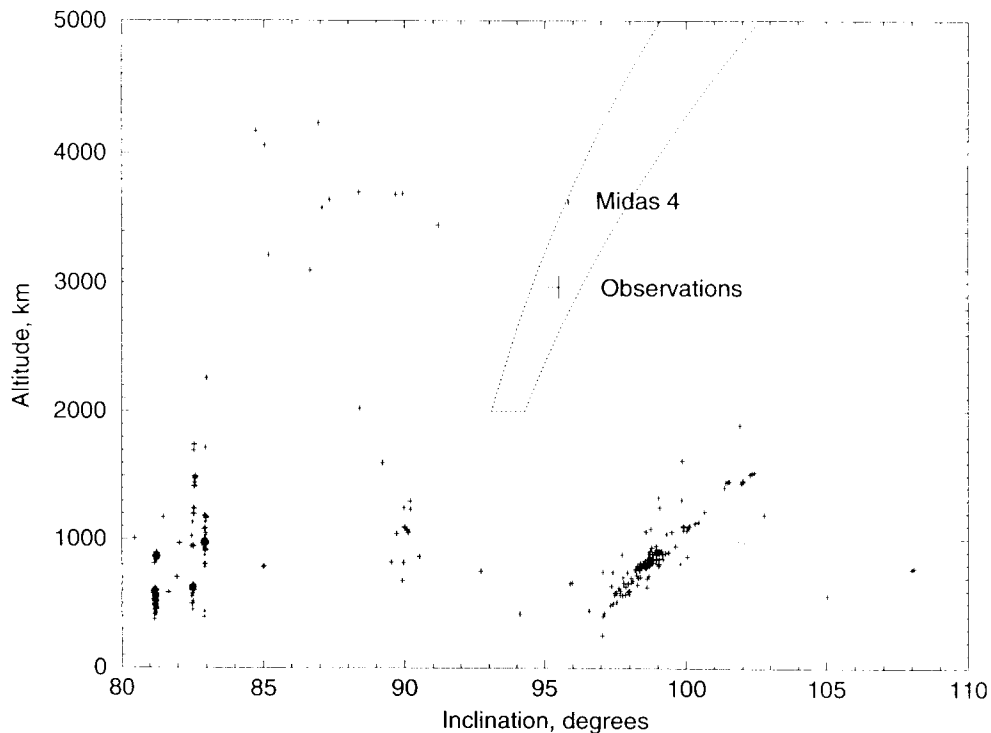


Fig. 6. Plot of Altitude vs Inclination of satellites now in Earth orbit. Only Midas 4 is close to the observations, indicating it is the source of the debris

communication experiment. Each dipole was 1.77 cm long and 0.00286 cm thick with an area to mass ratio of  $39.1 \text{ cm}^2 \text{ gm}^{-1}$ .

The orbit was carefully chosen so that an object of this area to mass ratio would reenter the Earth's atmosphere within 5 years due to perturbations caused by solar radi-

ation pressure. However, rather than orbit as individual needles, they stuck together, splitting into smaller lumps from time to time (Martin, 1967, page 86). Because of their much smaller area to mass ratio, the lumps did not reenter as planned.

The West Ford Project attempted the experiment again

in May, 1963. This time 400 million needles were launched, each 1.78 cm long and 0.00178 cm thick, leading to an area to mass ratio of  $62.7 \text{ cm}^2 \text{ gm}^{-1}$ . For this ratio, an orbit 3600 by 3700 km and  $87^\circ$  inclination satisfies the requirement that the needles reenter within 5 years. This time, all but 1/3 of them stuck together, and the experiment was declared a success. Even though some authors have maintained that all of the needles have reentered, new lumps of needles have been catalogued years after the West Ford Project (Shapiro 1966, Martin 1967 and Gabbard 1970).

The putative dipoles were manufactured to be resonant at the same wavelength as the Goldstone transmitter – 3.5 cm. This is not such a coincidence as may seem; the Goldstone and West Ford transmitters have a common heritage. We calculate that the radar cross section of a West Ford dipole is  $265 \text{ mm}^2$  when its axis is perpendicular to the line of sight. Such an orientation is unstable, however, as the gravity gradient effect favors a vertical alignment, which is along the line of sight. Thus most measurements would yield radar cross sections well below the maximum.

Only 0.1% of the objects in the first West Ford launch are required to obtain the 400,000 objects inferred from these observations. The fact that these objects are 650 km lower than the suggested launch vehicle, Midas 4, can be accounted for by the small amount of drag which exists, even at that altitude. For the last 5 years the semi-major axis of Midas 4 has been decreasing by 25 m per year (Molezan). It can be shown that the rate of decrease, for a fixed altitude, is proportional to the area to mass ratio. This ratio is 4 orders of magnitude greater for the dipoles, so the inferred altitude change could easily occur in several years.

Barsukov and Nazarova (1988) have reported that the flux of micrometeorites observed from the Elektron 1 and 3 spacecraft was maximum in the altitude range 3000 to 3500 km. These spacecraft, launched in 1964, were equipped with piezoelectric impact sensors, sensitive to impacts larger than  $10^{-7} \text{ gm}$ . The observations lasted 30 days. 51 impacts were detected, mostly between 3000 and 3500 km. This flux was attributed to a natural band of meteoric material. It seems unlikely, but not impossible, that these much smaller particles are associated with the ones we have observed near 2900 km.

## Summary and conclusions

We have obtained additional measurements of the altitudes and cross sections of the material in the near cluster. We have also made a statistical test of the polarization measurement at Haystack that confirms that there is much less power reflected when the received sense of circular polarization is the same as the transmitted sense. Consequently, we help confirm the previous interpretation that spherical droplets from the RORSAT vehicles are the particles of the near cluster.

The distant cluster of particles have radar cross sections

close to those expected for the West Ford dipoles. The inclination we found for the particle orbits agrees with only one spacecraft, that which launched the first set of West Ford dipoles. Although the altitude of the distant cluster is smaller than that of the spacecraft, the small drag forces which exist there are sufficient to account for the difference. We conclude that they are remnants of the 1961 West Ford launch.

We believe that most, if not all, of our observations are of human origin. It would be especially unusual for meteoritic or cometary particles to have such a well-defined, low eccentricity orbit and an inclination of  $96^\circ$  as does the distant cluster.

*Acknowledgements.* We thank the telescope operators at the Goldstone Tracking Station for their excellent support. The research described in this paper was carried out, in part, by the Jet Propulsion Laboratory, California Institute of Technology, under a contract with the National Aeronautics and Space Administration.

## References

- Barsukov, V. L. and Nazarova, T. N. (1988) Circular dust formations around earth and moon and some structural elements of dust formation around sun. *Astronomicheskii Vestnik* 61–70.
- Danby, J. M. A. (1962) *Fundamentals of Celestial Mechanics* The MacMillan Co., New York, 261.
- Gabbard, J. (1970) West Ford Needles Launch 1963 14. NORAD I4EDC Memorandum for Record 70–141, June 30, 1970.
- Goldstein, R. M. and Randolph, L. W. (1992) Rings of Earth. *IEEE Trans on Microwave Theory and Techniques* 40(6), 1077–1080.
- Goldstein, S. J. and Goldstein, R. M. (1994) Some Properties of Millimetric Space Debris. *The Astronomical Journal* 107(4), 367–371.
- Goldstein, R. M. and Goldstein, S. J. (1995) Flux of Millimetric Space Debris. *The Astronomical Journal* 110(3), 1392–1396.
- Johnson, N. L. (1993) United States space Surveillance. *Advances in Space Research* 13(8), 5–20.
- Kessler, D. J., Reynolds, R. C. and Anz-Meador, P. D. (1995) Current Status of Orbital Debris Models. 33<sup>rd</sup> Aerospace Sciences Meeting and Exhibit, Reno NV, paper no. AIAA 95-0662, Jan. 9–12, 1995.
- Mandeville, J. C. and Berthaud, L. (1995) From LDEF to EURECA – Orbital Debris and Meteoroids in Low-Earth Orbits. *Advances in Space Research* 16(11), 67–72.
- Martin, C. N. (1967) Satellites into Orbit. Translated by T. Schoeters, pp. 86–94. George G. Harrap & Co., LTD.
- Molezan, Anonymous FTP: kilroy.jpl.nasa.gov/pub/spaceelements/molezan
- Potter, A. E. (1995) Ground-Based Optical Observations of Orbital Debris – A Review. *Advances in Space Research* 16(11), 35–40.
- Shapiro, I. I. (1966) Last of the West Ford Dipoles. *Science* Vol. 154, no. 3755, 1445–1448.
- Stansbery, E. G., Bohannon, G., Pitts, C., Tracy, T. and Stanley, J. (1993) Radar Observations of Small Space Debris. *Advances in Space Research* 13(8), 43–48.
- Stansbery, E. G., Kessler, D. J. and Matney, M. J. (1995) Recent results of Orbital Debris Measurements from the Haystack Radar. 33<sup>rd</sup> Aerospace Sciences Meeting and Exhibit, Reno, NV, paper no. AIAA 95-0662, Jan. 9–12, 1995.